AD_____

Award Number: DAMD17-03-1-0146

TITLE: Apoptosis-Dependent and Apoptosis-Independent Functions of Bim in Prostate Cancer Cells

PRINCIPAL INVESTIGATOR: Dr. Dean Tang
Junwei Liu, M.D., Ph.D.

CONTRACTING ORGANIZATION: The University of Texas
MD Anderson Cancer Center
Smithville, TX 78957

REPORT DATE: March 2005

TYPE OF REPORT: Annual Summary

PREPARED FOR: U.S. Army Medical Research and Materiel Command
Fort Detrick, Maryland 21702-5012

# REPORT DOCUMENTATION PAGE

*Form Approved*
*OMB No. 0704-0188*



| 1. REPORT DATE | 2. REPORT TYPE | 3. DATES COVERED |
|---|---|---|
| 01-03-2005 | Annual Summary | 1 Mar 2003 – 28 Feb 2005 |

**4. TITLE AND SUBTITLE**

Apoptosis-Dependent and Apoptosis-Independent Functions of Bim in Prostate Cancer Cells

**5a. CONTRACT NUMBER**

**5b. GRANT NUMBER**
DAMD17-03-1-0146

**5c. PROGRAM ELEMENT NUMBER**

**6. AUTHOR(S)**
Dr. Dean Tang
Junwei Liu, M.D., Ph.D.

Email: dtang@mdanderson.org

**5d. PROJECT NUMBER**

**5e. TASK NUMBER**

**5f. WORK UNIT NUMBER**

**7. PERFORMING ORGANIZATION NAME(S) AND ADDRESS(ES)**

The University of Texas
MD Anderson Cancer Center
Smithville, TX 78957

**8. PERFORMING ORGANIZATION REPORT NUMBER**

**9. SPONSORING / MONITORING AGENCY NAME(S) AND ADDRESS(ES)**
U.S. Army Medical Research and Materiel Command
Fort Detrick, Maryland 21702-5012

**10. SPONSOR/MONITOR'S ACRONYM(S)**

**11. SPONSOR/MONITOR'S REPORT NUMBER(S)**

**12. DISTRIBUTION / AVAILABILITY STATEMENT**
Approved for Public Release; Distribution Unlimited

**13. SUPPLEMENTARY NOTES**
Original contains colored plates: ALL DTIC reproductions will be in black and white.

**14. ABSTRACT**

Attenuated apoptotic response and extended cell survival have been implicated in prostate cancer (PCa) development and progression. We recently found that Bim, a BH3-only pro-apoptotic protein, is upregulated in PCa cells in vitro and in vivo. The main objective of this post-doctoral fellowship is to elucidate why PCa cells upregulate Bim and what is the role of the upregulated Bim proteins in modulating PCa cell behavior (death, survival, proliferation/division, etc). Our hypothesis is that, under normal, unstimulated conditions, with its apoptotic function blocked, the upregulated Bim in PCa cells play an apoptosis-independent function(s). Under apoptosis-stimulated conditions, however, Bim can still participate in triggering a robust apoptotic response, thus guaranteeing that "weaker" or "more susceptible" PCa cells be eliminated from the population. Two Specific Aims were proposed to determine: 1) apoptosis-independent functions of the upregulated Bim in PCa cells under unstimulated conditions, and 2) apoptosis-dependent functions of the upregulated Bim in PCa cells under stimulated conditions. The PI of the grant, Dr. Junwei Liu, had to leave the lab Oct. of 2004. Before he left, he had completed all experiments in Specific Aim 2 with one manuscript published (Append. I). After he left, with the small amounts of funds left over from the Fellowship, we have just accomplished all of the experiments proposed in Specific Aim 1 and are in the process of preparing a manuscript, which will be supplied to DOD when it is ready.

**15. SUBJECT TERMS**
Prostate cancer, apoptosis, Bcl-2, Bim

| 16. SECURITY CLASSIFICATION OF: | | | 17. LIMITATION OF ABSTRACT | 18. NUMBER OF PAGES | 19a. NAME OF RESPONSIBLE PERSON |
|---|---|---|---|---|---|
| a. REPORT | b. ABSTRACT | c. THIS PAGE | | | USAMRMC |
| U | U | U | UU | 21 | 19b. TELEPHONE NUMBER *(include area code)* |

**Standard Form 298 (Rev. 8-98)**
**Prescribed by ANSI Std. Z39.18**

# TABLE OF CONTENTS

# Introduction

Attenuated apoptotic response and extended cell survival have been implicated in prostate cancer (PCa) development and progression. We recently found that Bim, a BH3-only pro-apoptotic protein, is upregulated in PCa cells *in vitro* and *in vivo*. The main objective of this post-doctoral fellowship is to elucidate why PCa cells upregulate Bim and what is the role of the upregulated Bim proteins in modulating PCa cell behavior (death, survival, proliferation/division, *etc*). Our hypothesis is that, under normal, unstimulated conditions, with its apoptotic function blocked, the upregulated Bim in PCa cells play an apoptosis-independent function(s). Under apoptosis-stimulated conditions, however, Bim can still participate in triggering a robust apoptotic response, thus guaranteeing that "weaker" or "more susceptible" PCa cells be eliminated from the population. Two Specific Aims were proposed to determine: 1) **apoptosis-independent functions of the upregulated Bim in PCa cells under unstimulated conditions, and 2) apoptosis-dependent functions of the upregulated Bim in PCa cells under stimulated conditions**.

***The PI of the grant, Dr. Junwei Liu, had to leave the lab Oct. of 2004. Before he left, he had completed all experiments in Specific Aim 2 with one manuscript published (Append. I). After he left, with the small amounts of funds left over from the Fellowship, we have just accomplished all of the experiments proposed in Specific Aim 1 and are in the process of preparing a manuscript***.

# Body

In the Statement of Work, we proposed the following two tasks.

***Task 1. To study apoptosis-independent functions of Bim in PCa cells (Months 1-16).***

*1). Subcellular localization and colocalization studies using confocal fluorescence microscopy*

*2). Subcellular localization and colocalization studies using biochemical and proteomic approaches*

*3. Gain-of-function studies in MDA 2b cells*

*4. Loss-of-function studies in PC3 and LNCaP cells*

***Outcome:*** We have accomplished both subaim 1 and subaim 2 now. As illustrated in Figure 1, both biochemical and fluorescence microscopy studies demonstrate that the Bim protein in PCa cells (shown in A are PPC-1 cells and in B PC3 cells; similar results have been obtained with several other PCa cell types) is distributed in multiple subcellular locations, in particular, in the membrane fractions (LM and HM) and in association with cytoskeleton. It is not expressed in the cytosol or nucleus.

Further co-localization studies demonstrate that Bim in PCa cells is associated with the LC8 dynein motor complex (Fig. 1B). These results suggest that the Bim protein constitutively expressed in PCa cells might be participating in biological functions associated with motor complex transport and cytoskeletal integrity.

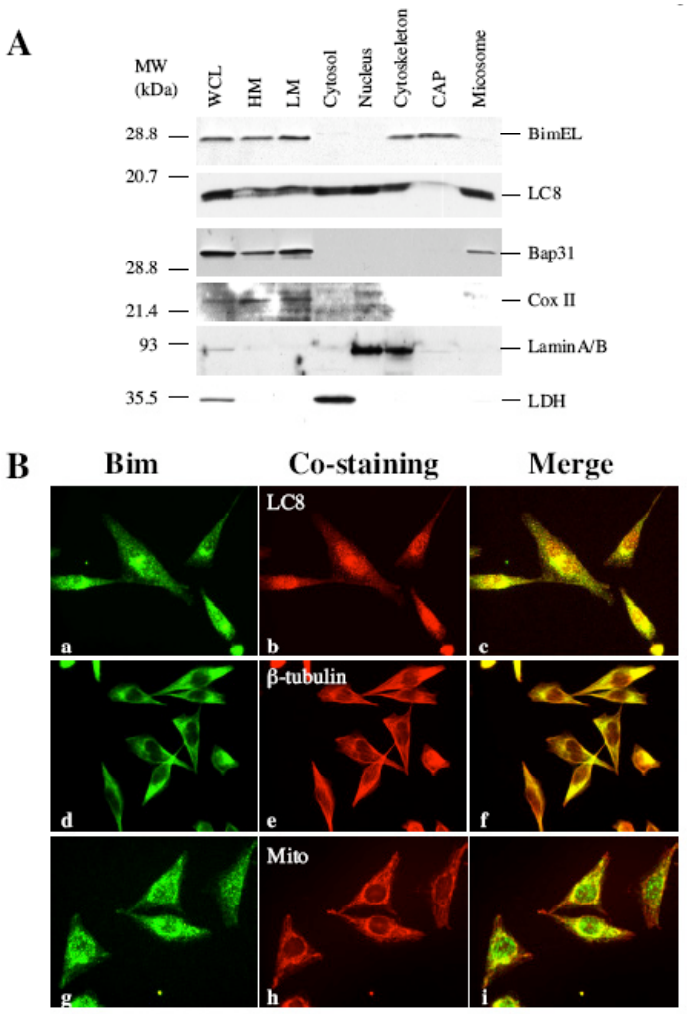


***Figure 1. Subcellular distribution studies of Bim in PCa cells.*** *(**A**). PPC-1 cells (5 x $10^7$) were subjected to subcellular fractionation and equal amounts of proteins (50 μg/lane) were separated on 15% SDS-PAGE and used in Western blotting. The individual fractions are indicated on the top and the probed molecules on the right. WCL, whole cell lysate; HM, heavy membrane; LM, light membrane; CAP, cytoskeleton-associated protein; Cox II, cytochrome c oxidase subunit II; LDH, lactate dehydrogenase. Bim was detected using the rabbit pAb. LC8 and LDH were detected using the antibodies described in Fig. 1A. Other antibodies used were: rabbit pAb to Bap31, mAb to Cox II (clone 12C4; Molecular Probes), and mixed goat pAb to lamin A and lamin B (Santa Cruz).. (**B**). Immunostaining of Bim using the pAb.*

For subaim 3, i.e., gain-of-function studies in MDA 2b PCa cells, we have established the stable clones and cells, as expected, showed a more aggressive phenotype in that they proliferated faster in vitro and were more tumorigenic in vivo.

For subaim 4, we have used siRNAs to knockdown Bim expression in multiple PCa cells. We first synthesized 3 double-stranded siRNAs (termed bim10, bim44, and bim122) targeted to different regions of the *bim* mRNA using the *Silencer*$^{TM}$ kit. The individual scrambled siRNAs were used as respective controls in the transfection experiments. When transfected into PPC-1 (Fig. 2A) or PC3 cells (not shown), these siRNAs downregulated the BimEL protein expression in a dose- and time-dependent manner. These *bim* siRNAs generally lost their silencing effects at ~72 h after transfection. We subsequently obtained a pool of 4 *bim* siRNAs from Dharmacon, which generally has longer-lasting and more potent silencing effects. As shown in Fig. 2B, the *bim* siRNA pool at 40 nM showed a time-dependent donwregulation of BimEL protein compared with the control siRNAs. In all 3 PCa cell lines examined, the BimEL protein decreased to barely detectable levels (Fig. 2B). The silencing effect was still complete by 7 days and only started to decline after 12 days (not shown). Dose studies revealed a silencing effect at 5 nM (not shown).

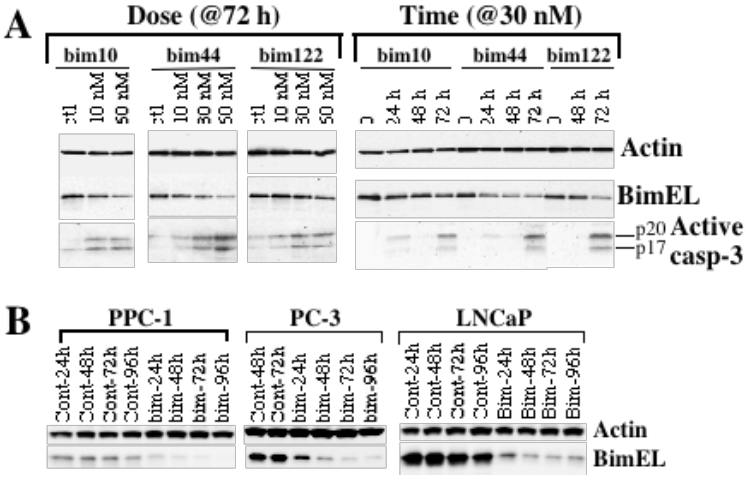


***Figure 2. Bim downregulation.*** *(**A**) Dose studies and time course of bim siRNA-induced BimEL downregulation and caspase-3 activation. PPC-1 cells (7 x 10$^4$ cell/well) were treated with 3 different Bim siRNAs, i.e., bim10, bim44, and bim122 (sequences not shown due to space constraint) at the concentrations or time intervals indicated. "Control" (ctl) refers to 60 nM of the respective scrambled control siRNAs. 25 μg whole cell lysate was used in Western blotting of the molecules indicated. The p20 and p17 bands represent active caspase-3 cleavage products. (**B**) PCa cells (PPC-1, PC3, or LNCaP) were transfected with 40 nM of the bim siRNA pool or control siRNAs for the time intervals indicated. 60-μg whole cell lysate was used in Western blotting.*

Much to our surprise, in all these siRNA experiments, we observed that downregulation of Bim caused a significant number of PCa cells to first round up and then detach (Fig. 3; next page), followed by anoikis and apoptosis as evidenced by typical apoptotic morphology (Fig. 3A and B), caspase-3 activation (Fig. 2A; bottom panels), and condensed and fragmented nuclei upon DAPI staining (not shown). Compared to the control siRNA pool, the *bim* siRNA pool induced time- (Fig. 3C) and dose-dependent increases in floating cells. As a consequence, the *bim* siRNA-transfected cultures contained much less live cells at the end of the experiments (see Fig. 3A and B for examples). For instance, 72 h after transfection of the control siRNA pool (40 nM) in PPC-1 cells, we generally obtained an increase in cell number by ~350-450%. By contrast, 72 h after transfecting the *bim* siRNAs (40 nM), we obtained ~33-45% of the initially plated cells.

**These loss-of-function experiments (Fig. 2-3) provide convincing evidence that the constitutively overexpressed Bim in PCa cells plays an important physiological function**, which is the central hypothesis of our grant.

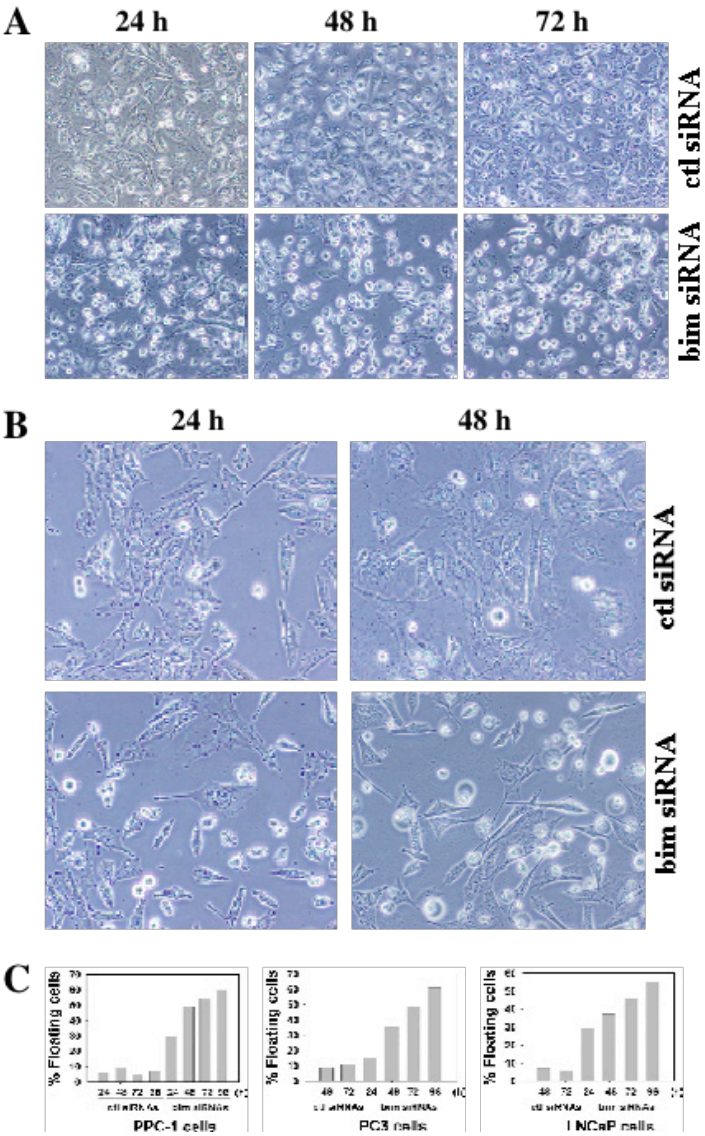


***Figure 3. Bim downregulation causes cell rounding, detachment, and apoptosis.*** *(**A**) PC3 cells were transfected with either the bim siRNA pool (bottom) or control (ctl) siRNA pool. Shown are representative microphotographs at various time intervals after transfection (x200). (**B**) PPC-1 cells were transfected with either the bim or ctl siRNA pool. Shown are representative micrographs at various time intervals after transfection (x200). (**C**) PCa cells were transfected with 40 nM of the bim siRNA pool or control (ctl) siRNAs for the time intervals indicated. The round and floating cells were enumerated at each time point and the results were expressed as the % floating cells in the*

***Task 2. To study apoptosis-dependent functions of upregulated Bim in PCa cells under apoptosis-stimulated conditions (Months 17-24)***

*1). Bim as an initiator of apoptosis in PCa cells*

*2). LNCaP cells subjected to serum starvation*

***Outcome***: By now we have accomplished both Subaims. Specifically, we have completed Specific Aim 2 with one manuscript published (Oncogene 24, 2020-2031, 2005; *Append.*). In this paper, using several apoptotic models, we demonstrate the importance of Bim in inducing PCa cell apoptosis. More importantly, we take one step further (than originally proposed) to elucidate how the Bim gene expression is upregulated at the molecular levels in these apoptotic models. We also put Bim induction in the context of general antagonistic prosurvival and prodeath signaling networks. This manuscript has important general implications in cancer cell response to various anti-cancer therapeutics.

# Key Research Accomplishments

1) Bim plays a key role in initiating apoptosis of PCa cells as well as many other cancer cells: it is transcriptionally induced early time on and its induction causally contributes to apoptosis induction.
2) The transcriptional induction of Bim represents one aspect of a global response of stimulated cells and is coupled to the simultaneous induction of multiple prosurvival mechanisms by apoptotic stimuli. The implication relating to cancer therapy is that the anti-tumor therapeutics will kill (prostate) cancer cells when, and *only when*, the prosurvival mechanisms are eliminated or overwhelmed by proapoptotic mechanisms.
3) In addition to its well-established roles in initiating cell death, Bim also possesses apoptosis-independent functions: siRNA-mediated ablation of Bim expression in PCa cells induces cell rounding, detachment, followed by cell death. In unstimulated PCa cells, constitutively overexpressed Bim associates with the microtubule cytoskeleton and microtubule-based motor complexes and this association appears to play a significant role in maintaining PCa cell cytoskeletal integrity and well being.
4) These studies establish a novel paradigm, i.e., cancer cells, including PCa cells, may utilize a prodeath molecule for multiple purposes, one of which is to help maintaining the well being of PCa cells.

# Future Plans

The current Fellowship project has come to an end. However, our lab will continue to explore the biological functions of Bim in regulating prostate cancer development.

# Reportable Outcomes

**Publication**

Liu, J-W., Chandra, D., Rudd, M.D., Butler, A.P., Pallotta, V., Brown, D., Coffer, P.J., and Tang, D.G**.** Induction of pro-survival molecules by apoptotic stimuli: Involvement of FOXO3a and ROS. ***Oncogene*** 24, 2020-2031, 2005.

# Conclusions

Overall the Fellowship project proceeded as we initially hypothesized, with all experiments proposed accomplished within 2 years. The project experienced a slight "bump" due to the unexpected and untimely departure of the PI but with the support of the small amounts of left-over fellowship funds we have accomplished the rest of the proposal. Our work strongly supports the dual-function model we proposed with regard to the roles of Bim in PCa development and progression. The findings we have made not only greatly enhance our understanding of how PCa cells may usurp normal apoptotic machinery molecules for their own survival and well being but also establish a new paradigm in which the conventionally thought, a BH-only proapoptotic Bcl-2 family protein can have an apoptosis-independent or even a pro-survival function.

# References

N/A

# Appendix Material

Liu, J-W., Chandra, D., Rudd, M.D., Butler, A.P., Pallotta, V., Brown, D., Coffer, P.J., and Tang, D.G**.** Induction of pro-survival molecules by apoptotic stimuli: Involvement of FOXO3a and ROS. ***Oncogene*** 24, 2020-2031, 2005.

Oncogene (2005) 24, 2020–2031

www.nature.com/onc

# Induction of prosurvival molecules by apoptotic stimuli: involvement of FOXO3a and ROS

Jun-Wei Liu[1], Dhyan Chandra[1], Michael D Rudd[1], Andrew P Butler[1], Vincent Pallotta[2], David Brown[2], Paul J Coffer[3] and Dean G Tang*[,1]

[1]*Department of Carcinogenesis, the University of Texas MD Anderson Cancer Center, Science Park-Research Division 1C, Smithville, TX 78957, USA;* [2]*Ambion, Inc., 2130 Woodward, Austin, TX 78744, USA;* [3]*Department of Pulmonary Diseases, University Medical Center, 3584 CX Utrecht, Netherlands*

**Most cancer therapeutics fails to eradicate cancer because cancer cells rapidly develop resistance to its proapoptotic effects. The underlying mechanisms remain incompletely understood. Here we show that three representative apoptotic stimuli, that is, serum starvation, a mitochondrial toxin, and a DNA-damaging agent (etoposide), rapidly induce several distinct classes of prosurvival molecules, in particular, Bcl-2/Bcl-$X_L$ and superoxide dismutase (SOD; including both MnSOD and Cu/ZnSOD). At the population level, the induction of these prosurvival molecules occurs prior to or concomitant with the induction of proapoptotic molecules such as Bim and Bak. Blocking the induction using siRNAs of the prosurvival or proapoptotic molecules facilitates or inhibits apoptosis, respectively. One master transcription factor, FOXO3a, is involved in the transcriptional activation of some of these prosurvival (e.g., MnSOD) and proapoptotic (e.g., Bim) molecules. Interestingly, in all three apoptotic systems, FOXO3a itself is also upregulated at the transcriptional level. Mechanistic studies indicate that reactive oxygen species (ROS) are rapidly induced upon apoptotic stimulation and that ROS inhibitors/scavengers block the induction of FOXO3a, MnSOD, and Bim. Finally, we show that apoptotic stimuli also upregulate prosurvival molecules in normal diploid human fibroblasts and at subapoptotic concentrations. Taken together, these results suggest that various apoptotic inducers may rapidly mobilize prosurvival mechanisms through ROS-activated master transcription factors such as FOXO3a. The results imply that effective anticancer therapeutics may need to combine both apoptosis-inducing and survival-suppressing strategies.**
*Oncogene* (2005) **24,** 2020–2031. doi:10.1038/sj.onc.1208385
Published online 24 January 2005

**Keywords:** apoptosis; Bim; Bcl-2; ROS; FOXO3a; MnSOD; cancer therapy

*Correspondence: DG Tang; E-mail: dtang@sprd1.mdacc.tmc.edu
Received 9 August 2004; revised 6 October 2004; accepted 19 November 2004; published online 24 January 2005

## Introduction

During development and tissue homeostasis, cell proliferation and cell death (apoptosis) are finely tuned and balanced in a social context so that a cell survives and proliferates only when it is needed to (Raff, 1992). Disruption of this balance and abnormal apoptosis can lead to developmental defects and contribute to various pathological conditions such as neurodegenerative and autoimmune diseases as well as cancer.

Apoptosis is normally suppressed by survival signals derived from neighboring cells (Raff, 1992). A major survival signal results from the activation of PI3K/Akt pathway. In the absence of survival signals, cells initiate apoptosis. Similarly, in response to stresses or toxins, cells also undergo apoptosis. Apoptosis is tightly regulated by the Bcl-2 family of proteins, which comprises anti- and pro-apoptotic members that contain one or more BH (i.e., BH1–BH4) domains (Danial and Korsmeyer, 2004). One group of proteins possesses only the BH3 domain, hence the name BH3-only proteins. The BH3-only Bcl-2 proteins are initiators of apoptosis – early in apoptosis they are either transcriptionally induced or post-transcriptionally activated and then rapidly targeted to the mitochondria to induce Bax, Bak-dependent release of proapoptotic molecules. In contrast, the antiapoptotic proteins (Bcl-2, Bcl-$X_L$, etc.) generally function by blocking the effects of the proapoptotic molecules.

Although great progress has been made in elucidating the core apoptotic machinery, we still have incomplete understanding of how cells initially respond to apoptotic stimulation. For example, when a population of cycling cells is stimulated by an apoptotic signal, do they immediately enter the apoptotic mode or do they first mobilize a defensive response? Or do the cells simultaneously activate both prosurvival and prodeath mechanisms in response to apoptotic stimuli and it is the balance between these two antagonizing signals that ultimately determines when and whether the stimulated cells will die? We recently find that many apoptotic stimuli cause an early mitochondrial activation characterized by a rapid induction of respiration-related proteins, including cytochrome *c* oxidase and apocytochrome *c*, the latter of which is then rapidly imported

into the mitochondria to participate in the mitochondrial respiration, leading to early membrane hyperpolarization, increased oxygen consumption, and maintenance of ATP levels (Joshi *et al*., 1999; Chandra *et al*., 2002). All these responses precede the exodus of holo-cytochrome *c* from mitochondria (Chandra *et al*., 2002). These observations point to the possibility that cells, upon apoptotic stimulation, perhaps rapidly mobilize defensive mechanisms in order to extend their survival. In this study, we test this possibility using three prototypical apoptotic stimuli and explore the underlying signaling mechanisms.

## Results

### *Three distinct apoptotic stimuli induce both proapoptotic and prosurvival molecules early during stimulation: common induction of Bim*

To test whether apoptotic stimuli might also induce prosurvival molecules, we employed three apoptotic inducers: serum deprivation to inactivate PI3K/Akt survival signaling, a DNA-damaging agent etoposide (VP16), and a mitochondrial toxin (BMD188) whose proapoptotic effect requires the mitochondrial respiratory chain (MRC) (Tang *et al*., 1998; Joshi *et al*., 1999; Chandra *et al*., 2002, 2004). We first determined their effects on proapoptotic Bcl-2 family proteins, in particular, the BH3-only protein Bim and multi-BH-domain proteins Bax and Bak. The reason that we focused on Bim, among multiple BH3-only proteins, is that Bim has recently emerged as a critical initiator of apoptosis (Dijkers *et al*., 2000; Putcha *et al*., 2001; Bouillet *et al*., 2002; Gilley *et al*., 2003).

As shown in Figure 1, Bim was induced in all three apoptotic systems – LNCaP prostate cancer cells subjected to serum starvation (a), SV40-transformed GM701 fibroblasts treated with BMD188 (b), and MDA-MB231 breast cancer cells treated with VP16 (c). At the population level, Bim induction took place prior to cell death and caspase-3 activation (Figure 1a–c). Bim induction in starved LNCaP (Figure 1a) and BMD188-treated GM701 (Figure 1b) cells was bell-shaped, with its levels going down at later time points, perhaps due to massive cell death. By contrast, Bim induction in VP16-stimulated MDA-MB231 cells was continuous, reaching a maximum 3 days (d) after stimulation (Figure 1c). In all three apoptotic systems, the induced Bim concentrated exclusively on the mitochondria (Figure 1a–c). In VP16-treated MDA-MB231 cells, all three major Bim isoforms (i.e., BimEL, BimL, and BimS) were induced (Figure 1c), whereas in serum-starved LNCaP and BMD188-treated GM701 cells BimEL was most prominently induced (Figure 1a and b). In contrast to Bim, another BH3-only protein, Bad, was slightly decreased in VP16-stimulated MDA-MB231 cells (Figure 1c).

Bax and Bak showed different responses. Bak was induced and expressed only on mitochondria in both starved LNCaP (Figure 1a) and BMD188-treated GM701 (Figure 1b) cells. In LNCaP cells, BAK induction peaked at 4 d upon deprivation and declined thereafter (Figure 1a), whereas in BMD188-treated GM701 cells BAK was continuously induced (Figure 1b). Bax was undetectable in LNCaP cells (not shown). In GM701 cells, Bax, which was mostly in the cytosol, showed increased translocation to the mitochondria at 15–30 min after BMD188 treatment and decreased thereafter in both compartments (Figure 1b), perhaps due to proteolytic degradation. By contrast, Bax was upregulated in the mitochondria of VP16-treated MDA-MB231 cells, while the levels of Bak, which also localized exclusively on mitochondria, did not significantly change (Figure 1c). These results suggest that, at the population level, all three types of apoptotic stimuli upregulated both Bim and Bak or Bax prior to caspase-3 activation.

In addition to Bim and Bax or Bak, we observed that the cytochrome *c* levels in both mitochondria and the cytosol were upregulated in all three apoptotic systems (Figure 1a–c). At earlier time points, the increased cytochrome *c* in the cytosol resulted partly from the newly synthesized apocytochrome *c* and partly from the released holocytochrome *c* as revealed by antibodies that differentiate between apo- and holocytochrome *c* (Chandra *et al*., 2002). For example, in LNCaP cells serum-starved for 2 d, some holocytochrome *c* was detected in the cytosol but more total cytochrome *c* was detected in the cytosol using the antibody that recognizes both apo- and holocytochrome *c* (Figure 1a), suggesting increased cytochrome *c* synthesis early during apoptosis induction. RT–PCR analysis also revealed increased cytochrome *c* levels early after serum withdrawal (not shown). At later time points, increased holocytochrome *c* was observed in the mitochondria (Figure 1a).

Since apocytochrome *c* in the cytosol is a powerful inhibitor of apoptosome-mediated caspase-9 activation and cell death (Martin and Fearnhead, 2002) and holocytochrome *c* in the mitochondria both plays a critical role in electron transport to generate ATP and functions as an antioxidant in the mitochondria (Zhao *et al*., 2003), the early upregulation of apocytochrome *c* in the cytosol and accumulation of holocytochrome *c* in the mitochondria in our apoptotic systems suggest that these apoptotic stimuli probably induce an early activation of prosurvival mechanisms. To further test this idea, we examined the protein levels of Bcl-2 and Bcl-$X_L$, two important antiapoptotic Bcl-2 family proteins. As shown in Figure 1, serum starvation upregulated Bcl-$X_L$ (a), VP16 upregulated Bcl-2 (c), and BMD188 upregulated both (b). The upregulation of Bcl-2 and/or Bcl-$X_L$ occurred around the same time as when proapoptotic molecules were induced and both increases occurred prior to caspase-3 activation and cell death (Figure 1a–c). Bcl-2 was not detected in LNCaP cells and starvation did not induce its expression (not shown).

Collectively, the above observations suggest that, in response to apoptotic stimulation, cells not only activate

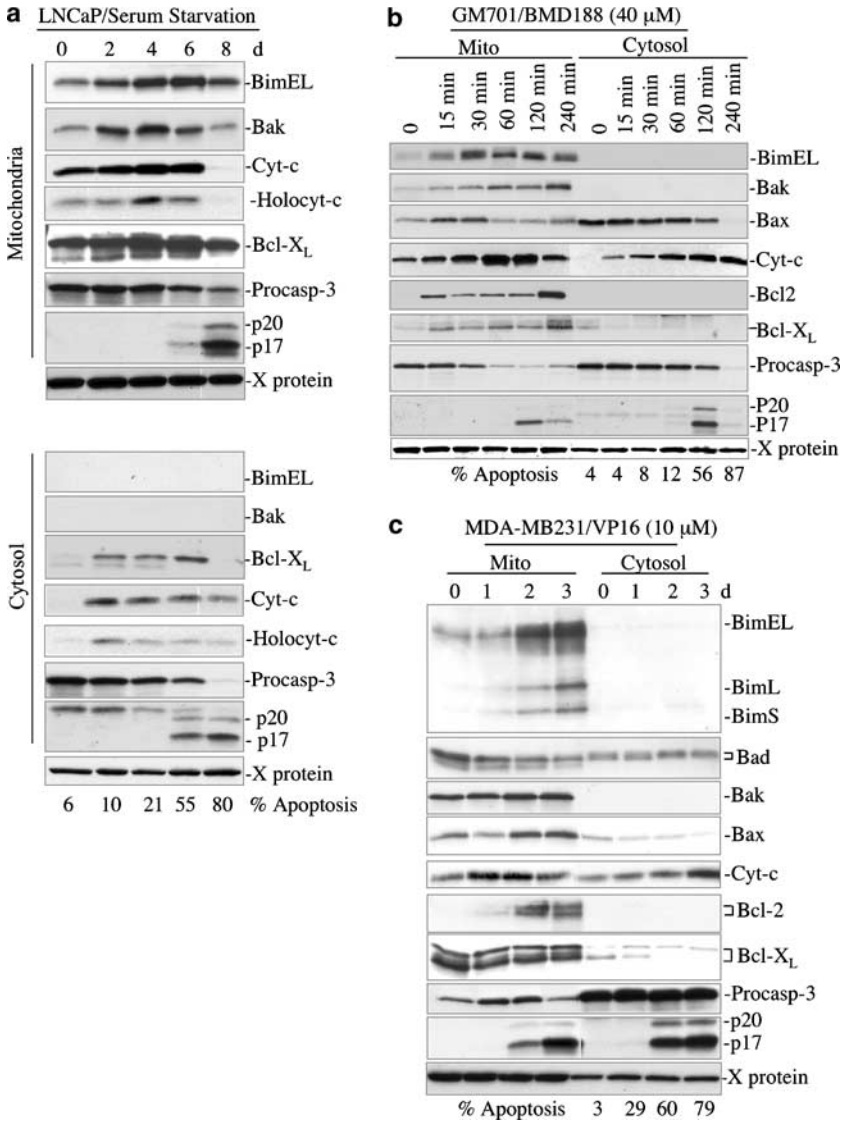


**Figure 1** Diverse apoptotic stimuli induce not only proapoptotic but also prosurvival molecules. Western blot analysis of mitochondrial and cytosolic fractions from LNCaP cells subjected to serum starvation (**a**), GM701 cells stimulated with BMD188 (**b**), or MDA-MB231 cells treated with VP16 (**c**). In all 30 $\mu$g of proteins from each sample was used and the blot was sequentially stripped and reprobed for the molecules indicated. The p20 and p17 were active caspase-3 bands. The X-protein, detected by the anti-cytochrome *c* (Cyt-c) antibody (Chandra *et al*., 2002), was used as a loading control. Note that the polyclonal anti-Bcl-$X_L$ antibody consistently detected two major bands in the MDA-MB231 cells (**c**) whereas a monoclonal anti-Bcl-$X_L$ antibody only detected the lower band in the same cells (see Figure 2d, inset). The % apoptosis (**a–c**) was determined by counting apoptotic nuclei upon DAPI staining

proapoptotic mechanisms but also activate prosurvival mechanisms.

*Suppression of Bim, or of Bcl-2 or Bcl-$X_L$ induction by RNAi delays or promotes early phases of apoptosis, respectively*

To determine the functional significance of the induction of both pro and anti-apoptotic Bcl-2 molecules, we employed siRNA to Bim, Bcl-2, or Bcl-$X_L$. As shown in Figure 2, Bim siRNA partially inhibited Bim induction and delayed apoptosis in BMD188-treated GM701 (2a) and VP16-treated MDA-MB231 (2b) cells. At later time points, Bim siRNA did not demonstrate significant inhibitory effects on apoptosis, probably because other apoptotic signals were also activated and/or because the Bim siRNA was degraded.

By contrast, Bcl-2 and Bcl-$X_L$ siRNAs partially inhibited the induction of their respective targets and also promoted BMD188-induced apoptosis in GM701 fibroblasts (Figure 2c). In MDA-MB231 cells, Bcl-$X_L$ was constitutively expressed at high levels and VP16 treatment did not significantly alter its expression (Figure 1c). Interestingly, downregulation of Bcl-$X_L$ by siRNA caused significant basal-level apoptosis and the combination of Bcl-$X_L$ siRNA with VP16 treatment further increased apoptosis (Figure 2d).

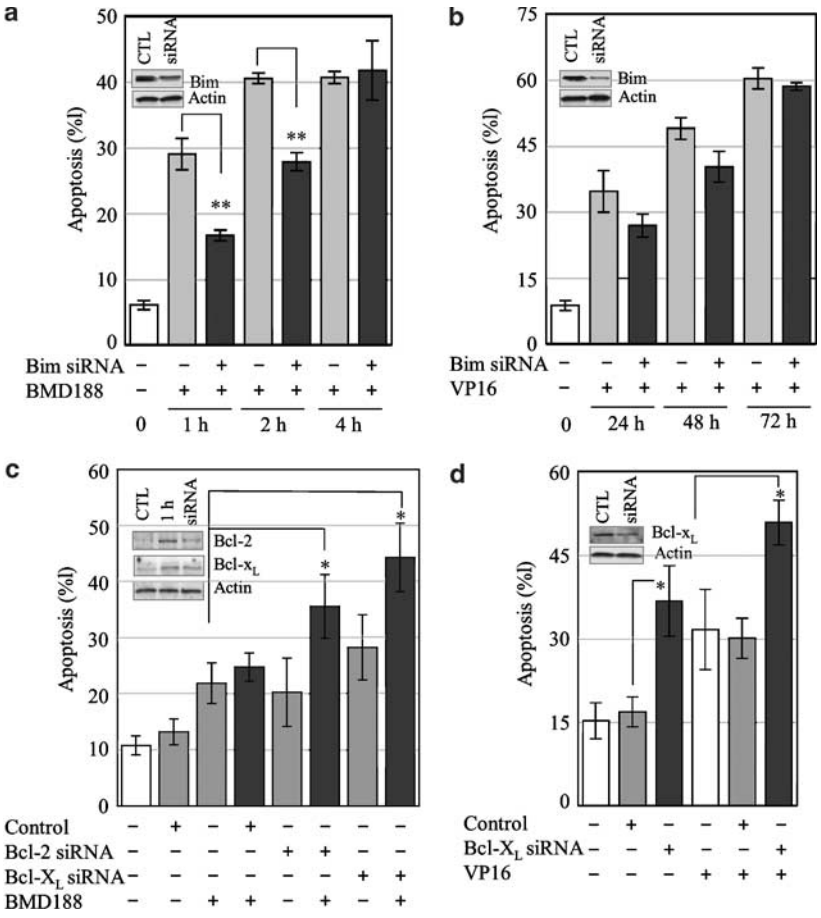


**Figure 2** Bim induction contributes to apoptosis induction and Bcl-2, Bcl-$X_L$ induction extends cell survival (**a, b**). Bim siRNA inhibits Bim induction and delays apoptosis. GM701 (**a**) or MDA-MB231 (**b**) cells were transfected with Bim siRNA (60 nM). After 24 h, cells were treated with BMD188 (40 $\mu$M; **a**) or VP16 (10 $\mu$M; **b**) for the time intervals indicated. At the end, cells were harvested for Western blotting (inset, 48 h after transfection) or scored for apoptosis. Note that Bim siRNA also reduced VP16-induced death of MDA-MB231 cells at 24 and 48 h post-treatment ($P<0.05$) (**b**). (**c, d**) Bcl-2 or Bcl-$X_L$ siRNA inhibits Bcl-2 or Bcl-$X_L$ induction and facilitates apoptosis. GM701 cells (**c**) or MDA-MB231 cells (**d**) were transfected with either Bcl-2 and/or Bcl-$X_L$ siRNA (100 nM). After 24 h, cells were treated with BMD188 (40 $\mu$M) for 1 h (**c**) or VP16 for 1 d (**d**). Then cells were harvested for Western blotting (inset, 48 h after transfection) or scored for apoptosis. *$P<0.05$; **$P<0.01$ (Student's *t*-test)

These results altogether suggest that Bim and Bcl-2/Bcl-$X_L$ induced by apoptotic stimuli are causally involved in promoting cell death and survival, respectively. The results also suggest that in some cells such as MDA-MB231 endogenous expression of prosurvival molecules such as Bcl-$X_L$ is important in maintaining cell survival.

### *Superoxide dismutases (SODs) are also induced by apoptotic stimuli*

Next, we determined whether these apoptotic stimuli also affected another class of defense molecules, the SODs. There are two major types of SODs, the mitochondrial MnSOD and cytosolic Cu/ZnSOD, both of which function by removing reactive oxygen species (ROS), in particular, superoxide anions (Kinnula and Crapo, 2003; Mikkelsen and Wardman, 2003). As shown in Figure 3a, c and e, all three apoptotic stimuli upregulated the levels of both MnSOD and Cu/ZnSOD at around the same time when Bim was induced. To determine whether the upregulated SODs played a defensive role, we transfected MDA-MB231 cells with MnSOD siRNA prior to VP16 treatment. As shown in Figure 3g, transfection of the MnSOD siRNA significantly increased apoptosis, suggesting that the basal-level MnSOD expression in MDA-MB231 cells plays an important role in maintaining cell viability. VP16 treatment alone also induced obvious cell death (Figure 3g). Importantly, the MnSOD siRNA partially reduced the MnSOD induction and significantly enhanced the proapoptotic effect of VP16 (Figure 3g). These results together suggest that both the basal and the apoptotic stimuli-induced MnSOD plays a prosurvival function.

### *FOXO3a, a transcriptional activator of Bim and MnSOD, is also upregulated early during apoptosis induction*

The preceding experiments demonstrated that all three apoptotic stimuli induce not only proapoptotic

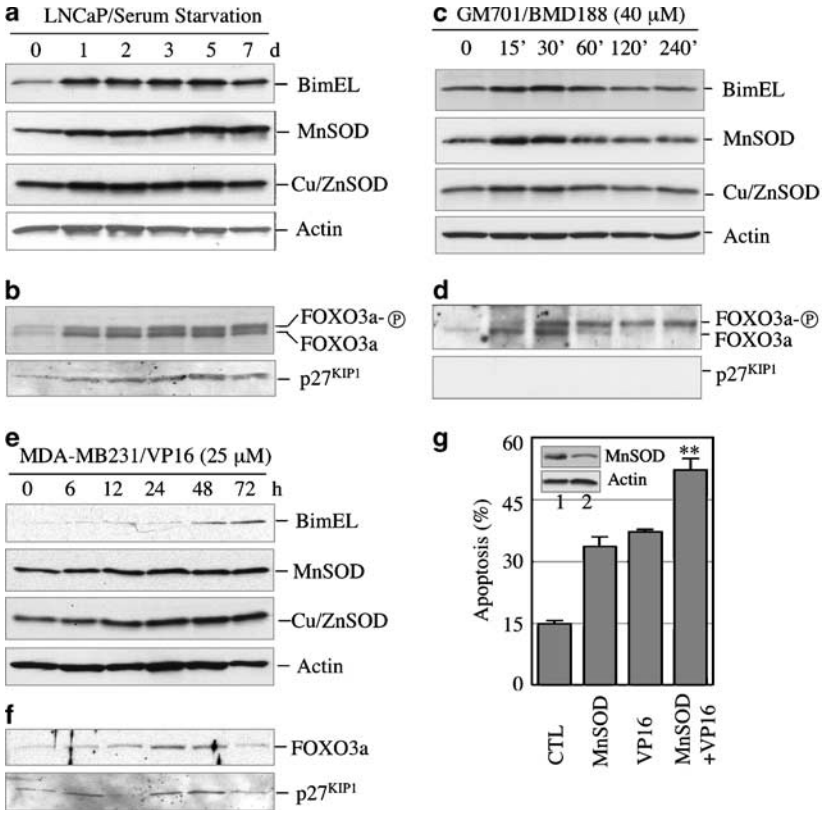


**Figure 3** Upregulation of FOXO3a and its transcriptional targets during apoptosis. Western blot analysis using whole-cell lysates (40 $\mu$g/lane) from serum-starved LNCaP cells (**a, b**), BMD188-treated GM701 cells (**c, d**), or VP16-treated MDA-MB231 cells (**e, f**) for the molecules indicated. In (b and d), FOXO3a was detected as both a lower band and an upper, perhaps phosphorylated form. (**g**) MnSOD siRNA partially inhibited induction of MnSOD and promoted VP16-induced cell death. MDA-MB231 cells were transfected with scrambled control (inset, lane 1; CTL) or MnSOD (inset, lane 2) siRNAs (both at 100 nM). After 48 h, cells were treated with VP16 (25 $\mu$M) for 24 h. $^{**}P<0.01$ (MnSOD + VP16 *vs* MnSOD or VP16)

(i.e., Bim, Bax, Bak) but also antiapoptotic (i.e., cytochrome *c*, Bcl-2, Bcl-$X_L$, MnSOD, Cu/ZnSOD) molecules. Which transcription factors might be responsible for the induction of these molecules? We reasoned that master transcription factors known to play critical roles in determining the life and death of a cell, such as p53, NF-$\kappa$B, E2F1, and FOXO3a, might be involved. We focused our initial efforts on FOXO3a because both Bim and MnSOD have previously been shown to be transcriptional targets of FOXO3a.

FOXO3a (FKHR-L1) is a mammalian homologue of *C. elegans* DAF-16 and one of the FOXO (Forkhead box, class O) subclass of Forkhead transcription factors (Birkenkamp and Coffer, 2003). FOXO3a plays a critical role in coordinating cell survival and death and regulating stress responses and longevity (Brunet *et al*., 1999; Birkenkamp and Coffer, 2003). The nonphosphorylated, active form of FOXO3a localizes to the cell nucleus where it functions as a transcriptional factor to effect either cell-cycle arrest or cell death, similar to p53. Survival factors or mitogens cause the phosphorylation of FOXO3a, which inhibits target gene transcription or promotes proteosome-mediated degradation (Plas and Thompson, 2003). FOXO3a transcriptionally downregulates cyclin D1 (Ramaswamy *et al*., 2002; Schimidt *et al*., 2002) and activates Bim (Dijkers *et al*., 2000; Birkenkamp and Coffer, 2003; Gilley *et al*., 2003), TRAIL (Modur *et al*., 2002), TRADD (Rokudal *et al*., 2002), MnSOD (Kops *et al*., 2002), and cyclin-dependent kinase inhibitor $p27^{KIP1}$ (Birkenkamp and Coffer, 2003).

Since both Bim and MnSOD were induced by the three apoptotic stimuli we used (Figures 1 and 3), we examined the levels of $p27^{KIP1}$, another FOXO3a target. As shown in Figure 3b, serum-starved LNCaP cells showed a time-dependent upregulation of $p27^{KIP1}$. VP16-treated MDA-MB231 cells similarly showed increased expression of $p27^{KIP1}$ (Figure 3f). GM701 cells expressed undetectable levels of $p27^{KIP1}$ protein (Figure 3d), although its mRNA levels increased upon BMD188 treatment (see Figure 5b, below).

The coordinated induction of all three FOXO3a targets – Bim, MnSOD, and $p27^{KIP1}$ – prompted us to examine the status of FOXO3a itself in our apoptotic systems. Interestingly, FOXO3a was also upregulated in all three systems, although with different characteristics (Figure 3b, d, and f). In serum-starved LNCaP cells, FOXO3a was upregulated as early as 1 d and the upregulated FOXO3a remained at about the same level for at least 5 d (Figure 3b). Increased levels of an upper band of FOXO3a were also detected (Figure 3b), which represented the phosphorylated FOXO3a, as revealed in

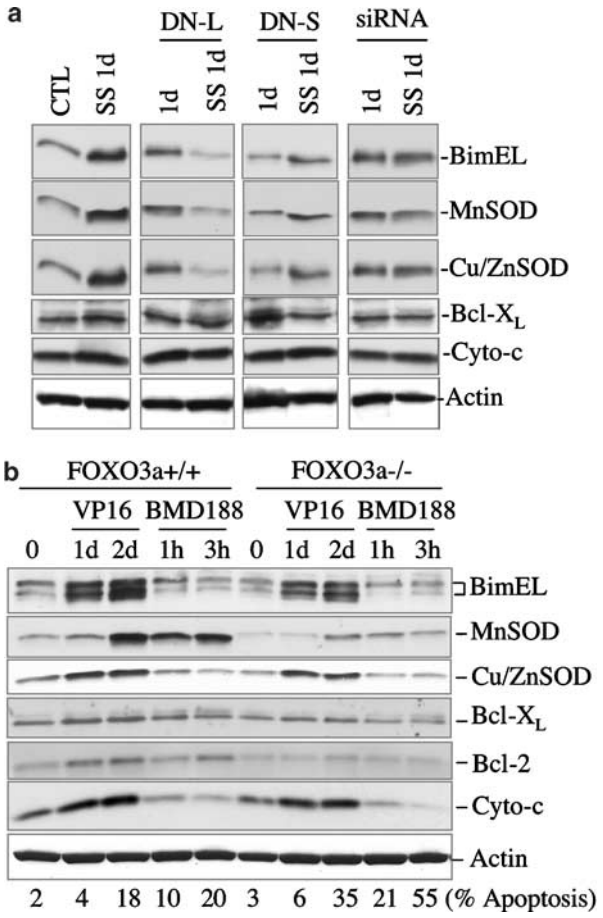


**Figure 4** Effects of FOXO3a DN constructs and siRNA on the induction of other molecules. (**a**) LNCaP cells were transfected with DN-L, DN-S, or siRNA of FOXO3a. After 24 h, cells were harvested for Western blotting. (**b**) FOXO3a$^{+/+}$ and FOXO3a$^{-/-}$ MEFs were treated with either VP16 (10 $\mu$M) or BMD188 (40 $\mu$M). At the end, cells were harvested for Western blotting or scored for apoptosis

preliminary Western blotting studies using an antibody that preferentially recognizes the phosphorylated FOXO3a (i.e., FOXO3a$^{T32}$) (not shown). In BMD188-treated GM701 cells, FOXO3a was induced by 15 min and reached the peak level by 30 min (Figure 3d). Surprisingly, FOXO3a appeared to be degraded after 30 min while the phosphorylated, inactive, FOXO3a started to accumulate (Figure 3d). In contrast, VP16 upregulated only the FOXO3a, which was induced at 12 h after treatment and the upregulation peaked at 24 h (Figure 3e). Together, these data suggest that FOXO3a, like its targets, is also upregulated early during apoptosis induction and, in some systems such as BMD188-treated GM701 cells, FOXO3a protein expression and activity seem to be tightly regulated.

To determine whether Bim and MnSOD are indeed FOXO3a targets in our cells, we utilized two dominant-negative (DN) constructs of FOXO3a (Dijkers *et al*., 2002), that is, FKHR DBD-L (DN-L) and FKHR DBD-S (DN-S), to inhibit the FOXO3a activity. We also utilized a FOXO3a siRNA to inhibit its induction. As shown in Figure 4a, serum starvation of LNCaP for 1 d induced both BimEL and MnSOD, as well as Cu/ZnSOD. Both DN FOXO3a constructs and FOXO3a siRNA inhibited, to different degrees, the induction of Bim and MnSOD (Figure 4a). The DN-L showed the strongest inhibitory effect in that it also decreased the basal-level expression of Bim and MnSOD (Figure 4a). Interestingly, starvation-induced upregulation of Cu/ZnSOD in LNCaP cells was also inhibited by FOXO3a DN constructs and siRNA (Figure 4a). We also determined the relationship between FOXO3a and Bcl-X$_L$ and cytochrome *c*. As shown in Figure 4a, 1 d deprivation slightly induced Bcl-X$_L$ and cytochrome *c*. As in the case of Cu/ZnSOD, DN FOXO3a and, in particular, FOXO3a siRNA also seemed to repress the induction of both molecules (Figure 4a).

To further explore the relationship between FOXO3a, its two known targets (i.e., MnSOD and Bim), and several other molecules, we treated FOXO3a$^{+/+}$ and FOXO3a$^{-/-}$ mouse embryonic fibroblasts (MEFs) (Castrillon *et al*., 2003) with VP16 or BMD188. As shown in Figure 4b, Bim, which was detected as two major bands, was strongly induced by VP16 in FOXO3a$^{+/+}$ cells but only partially induced in FOXO3a$^{-/-}$ cells. BMD188 did not upregulate the Bim proteins in these MEFs (Figure 4b). MnSOD was induced by both apoptotic stimuli in FOXO3a$^{+/+}$ cells, and the induction was completely suppressed in FOXO3a$^{-/-}$ cells (Figure 4b). Similar to Bim, Cu/ZnSOD was induced by VP16 but not by BMD188 (Figure 4b). The VP16-induced Cu/ZnSOD upregulation was also partially inhibited in FOXO3a$^{-/-}$ cells (Figure 4b). VP16, but not BMD188, also significantly upregulated cytochrome *c* and slightly upregulated Bcl-X$_L$ and Bcl-2 in FOXO3a$^{+/+}$ MEFs (Figure 4b). Interestingly, the induction of the three latter molecules was also reduced (cytochrome *c*) or inhibited (Bcl-2 and Bcl-X$_L$) in FOXO3a$^{-/-}$ MEFs (Figure 4b). Of importance, when FOXO3a$^{+/+}$ and FOXO3a$^{-/-}$ MEFs were compared for their apoptotic sensitivities, FOXO3a$^{-/-}$ cells were consistently found to be more susceptible than FOXO3a$^{+/+}$ cells to both death stimuli (Figure 4b).

### *Transcriptional upregulation of FOXO3a and other molecules*

Next, we carried out semiquantitative RT–PCR analysis to determine whether FOXO3a and other molecules are indeed induced at the transcriptional level. In LNCaP cells starved for 4 h to 7 d, FOXO3a mRNA slightly increased at 4–8 h upon withdrawal of serum (Figure 5a). The induction reached maximum level by 1 d, after which the levels stayed roughly the same (Figure 5a). The induction of Bim, MnSOD, and p27$^{KIP1}$ occurred around the same time as that of FOXO3a, and all peaked at $\sim$24 h except Bim, whose mRNA was maximally induced by 2 d and then declined (Figure 5a). In GM701 cells treated with BMD188, the mRNA levels of FOXO3a, Bim, p27$^{KIP1}$, and Bcl-2 were upregulated at $\sim$15 min and then continued to increase (Figure 5b). The induction of MnSOD and cytochrome *c* mRNAs appeared slightly slower, at

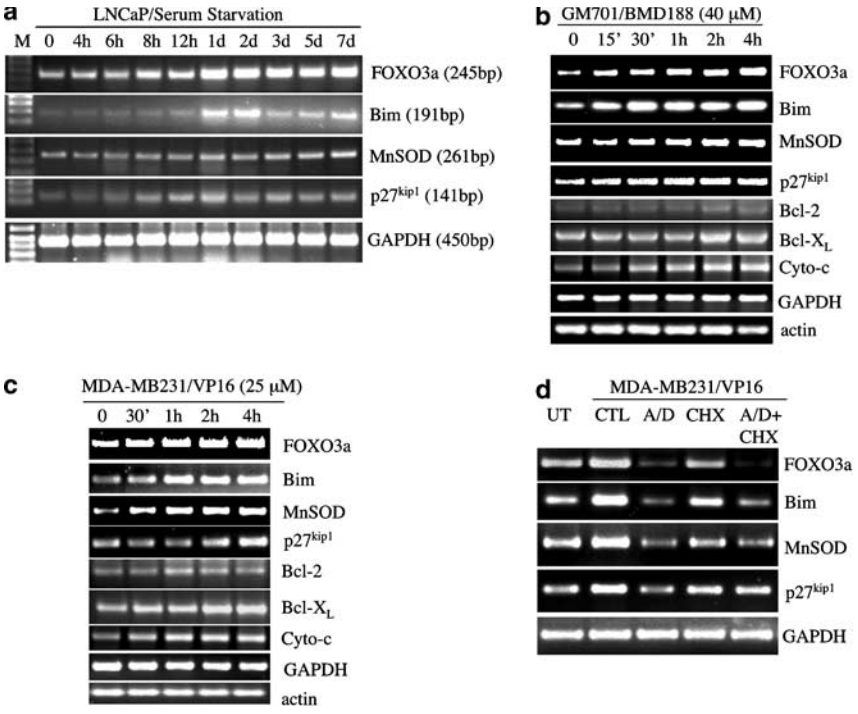


**Figure 5** Transcriptional upregulation by apoptotic stimuli of FOXO3a and other molecules. RT–PCR analysis in serum-starved LNCaP (**a**), BMD188-treated GM701 (**b**), and VP16-stimulated MDA-MB231 (**c**) cells. (**d**) MDA-MB231 cells were pretreated with actinomycin D (A/D, 1 nM), cycloheximide (CHX, 1 $\mu$M), or both for 1.5 h before apoptosis stimulation. UT, untreated; CTL, vehicle control

~30 min after treatment (Figure 5b). In contrast, the Bcl-$X_L$ mRNA was not significantly upregulated until at ~2 h after stimulation (Figure 5b), suggesting that the BMD188-induced Bcl-$X_L$ protein upregulation at earlier time points (Figure 1b) likely resulted from post-transcriptional mechanisms. In MDA-MB231 cells stimulated with VP16, as in the BMD188-stimulated GM701 cells, FOXO3a and all the other molecules examined showed upregulation in their mRNA levels but with varying kinetics (Figure 5c).

To determine whether the increased mRNAs of FOXO3a and Bim, MnSOD, and $p27^{KIP1}$ truly resulted from transcriptional activation, we pretreated MDA-MB231 cells with actinomycin D (A/D), which inhibits *de novo* RNA synthesis, or cycloheximide (CHX), which inhibits protein synthesis, or both, for 1 h before apoptosis stimulation. As shown in Figure 5d, the mRNA levels of FOXO3a, Bim, MnSOD, and $p27^{KIP1}$ were increased after apoptosis stimulation for 2 h. The mRNA upregulation of all four molecules was completely inhibited by A/D and partially by CHX. In fact, A/D inhibited even the basal-level transcription of all four molecules. The combination of A/D and CHX inhibited their mRNA levels very similarly to A/D alone. The inhibitory effect of CHX was likely due to its inhibition of some transcriptional machinery proteins.

### *Rapid ROS generation in all three apoptotic systems*

So how might FOXO3a itself be induced? Several lines of evidences made us think that ROS may be involved. First, in all three apoptotic systems there was early mitochondrial activation, characterized by increased holocytochrome *c* accumulation in the mitochondria, upregulated cytochrome *c* oxidase (i.e., complex IV) expression and activity, and mitochondrial inner membrane hyperpolarization (Joshi *et al*., 1999; Chandra *et al*., 2002). Mitochondria are the major organelles that produce ROS, and increased mitochondrial activity is generally accompanied by increased ROS generation (Mikkelsen and Wardman, 2003). Second, the prosurvival molecules induced by apoptotic stimuli, including cytochrome *c*, Bcl-2, Bcl-$X_L$, and SODs, are all related to ROS or oxidative stress. For example, holocytochrome *c* is an essential antioxidant in the mitochondria in that it both inhibits the generation of and scavenges superoxide and hydrogen peroxide ($H_2O_2$) (Zhao *et al*., 2003). Bcl-2 functions as an antioxidant (Hockenbery *et al*., 1993) and oxidative stress upregulates the expression of Bcl-$X_L$ (Valks *et al*., 2003) and Bim (Sade and Sarin, 2004). Third, ROS are well known to play dual functions in mediating mitogen or survival factor-signaled cell proliferation and survival and oxidative stress-induced cell death (Sundaresan *et al*., 1995; Adler *et al*., 1999; Huang *et al*., 2003; Mikkelsen and Wardman, 2003).

The main types of ROS include superoxide anion ($O_2^{\bullet -}$), hydroxyl radicals ($^{\bullet}OH$), and $H_2O_2$. To address whether ROS might be involved in upregulating FOXO3a and some of the other molecules, we first examined whether ROS were generated in our apoptotic systems. We used dihydroethidium (DHE) to measure

$O_2^{\bullet-}$ and dihydrorhodamine 123 (DHR123) to measure $H_2O_2$. As shown in Figure 6a and b, a time-dependent increase in $O_2^{\bullet-}$ was observed in all three apoptotic systems, and it occurred much earlier than the onset of apoptosis (Figure 1a–c). For example, increased $O_2^{\bullet-}$ was detected in BMD188-treated GM701 cells as early as 1 min and in VP16-stimulated MDA-MB231 cells within 4 h (Figure 6a and b). Interestingly, the levels of $O_2^{\bullet-}$ appeared to be correlated with the sensitivity of the cells to apoptosis induction. For example, BMD188 caused highest levels of $O_2^{\bullet-}$ (Figure 6a and b) and also induced maximum cell death within the shortest time (Figure 1b). By contrast, serum starvation generated lowest levels of $O_2^{\bullet-}$ (Figure 6a and b) and also caused the slowest apoptosis (Figure 1a). Measuring ROS generation using DHR also revealed increased $H_2O_2$ in these apoptotic systems (not shown).

In these experiments, increased ROS generation (Figure 6a and b) occurred prior to caspase-3 activation (Figure 1). To exclude the possibility that ROS generation was a consequence of caspase activation (Ricci *et al*., 2003), we treated GM701 cells with BMD188 in the presence of a general caspase inhibitor, zVAD-fmk (zVAD). As shown in Figure 6b (right panel), zVAD did not prevent increased ROS generation by BMD188, suggesting that the BMD188-caused ROS increase did not result from caspase activation.

### *Increased ROS are causally involved in upregulating FOXO3a and its targets*

To determine whether the increased ROS production is causally involved in regulating FOXO3a and its targets, we pretreated LNCaP cells with ROS inhibitors/scavengers, *N*-acetyl cysteine (NAC), mannitol, or GSH (Tang and Honn, 1997) prior to starvation. As shown in Figure 6c, all three ROS inhibitors suppressed starvation-induced upregulation of FOXO3a and its targets, BimEL and MnSOD. Interestingly, FOXO3a and MnSOD were induced as early as 8 h, which was inhibited by ROS scavengers (Figure 6c). By 24 h, FOXO3a and MnSOD were further induced, and the inhibitory effects of ROS scavengers slightly declined (Figure 6c), likely due to degradation of these chemicals. By contrast, Bim induction occurred slightly later, that is, ~24 h after the start of deprivation, but the ROS inhibitors similarly suppressed its induction (Figure 6c). Together, these results suggest that (1) FOXO3a and MnSOD are induced earlier than Bim in serum-deprived LNCaP cells; and (2) deprivation-induced expression of all three molecules can be suppressed by ROS inhibitors/scavengers.

To further establish the connection between ROS and FOXO3a and its targets, we carried out the opposite experiments: we treated serum-cultured LNCaP cells with ROS-generating reagents. As shown in Figure 6d, $H_2O_2$ treatment upregulated FOXO3a, Bim, and MnSOD.

### *Induction of FOXO3a and prosurvival and prodeath molecules in normal human diploid fibroblasts (NHDF) and at subapoptotic concentrations of stimuli*

Next, we examined whether the apoptotic stimuli-induced expression of prosurvival molecules was unique to transformed (GM701) or cancer (LNCaP and

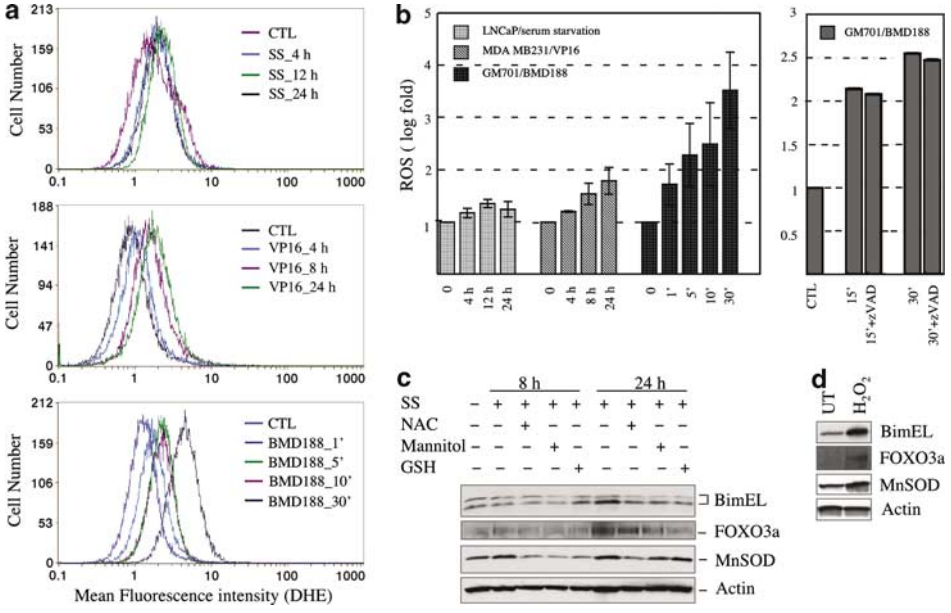


**Figure 6** ROS involvement in the induction of FOXO3a and its targets by apoptotic stimuli. (**a**) ROS levels in starved LNCaP cells, MDA-MB231 cells treated with VP16 (25 $\mu$M), and GM701 cells treated with BMD188 (40 $\mu$M). (**b**) Quantification of ROS levels (log fold). Values represent the mean ± s.d. from three experiments. In a separate experiment, GM701 cells were pretreated with *z*-VAD (1 $\mu$M × 1.5 h) before BMD188 treatment (right panel). (**c**). LNCaP cells were pretreated with NAC, mannitol, and GSH for 1.5 h before subjected to serum starvation (SS) for 8 or 24 h. At the end, cells were harvested for Western blotting of FOXO3a, MnSOD, or BimEL. Note that the faint band above the BimEL probably represents the phosphorylated Bim. (**d**) LNCaP cells were treated with $H_2O_2$ (1 mM) for 6 h. Cells were harvested for Western blotting of FOXO3a, MnSOD, Bim, or actin

MDA-MB231) cells and treated primary NHDF with VP16. As shown in Figure 7a and b, VP16 similarly upregulated FOXO3a and both prosurvival (i.e., Bcl-$X_L$, MnSOD, and Cu/ZnSOD) and prodeath (i.e., Bim, Bak, and Bax) molecules.

Finally, we asked whether this same spectrum of molecules could still be induced if the apoptotic stimulus was used at a very low concentration so that it does not induce cell death. VP16 was used in all the preceding experiments at 10–25 $\mu$M to induce cell death. When VP16 was used at 0.15 $\mu$M, no significant apoptosis was observed within a 5 d treatment period (Figure 7d). Nevertheless, Bcl-$X_L$ was induced as early as 1 d post-treatment (Figure 7c). By 2 d, FOXO3a, Bim, and Bak were upregulated (Figure 7c and d). Later, by 4 d, both Bax and Cu/ZnSOD were also induced (Figure 7c and d). The only exception was MnSOD, which was not induced throughout the treatment period (Figure 7d).

## Discussion

Our first finding in the present study is that apoptotic stimuli activate not only prodeath but also prosurvival molecules. At least five classes of prosurvival molecules are induced by apoptotic stimuli. The first class belongs to the molecules normally involved in mitochondrial respiration, including cytochrome *c* oxidase and cytochrome *c* (Joshi *et al*., 1999; Chandra *et al*., 2002). The upregulation of these MRC proteins perhaps represents one aspect of the global mitochondrial activation aimed to maintain critical ATP levels. Moreover, increased apocytochrome *c* in the cytosol and upregulated holocytochrome *c* in the mitochondria also serve antiapoptotic functions (Martin and Fearnhead, 2002; Zhao *et al*., 2003). The second class of prosurvival molecules induced or activated by apoptotic stimuli is antiapoptotic Bcl-2 family proteins, in particular, Bcl-2 and/or Bcl-$X_L$, which also function in mitochondria. The third class of prosurvival molecules is the SODs, including both mitochondrial MnSOD and cytosolic Cu/ZnSOD. The fourth class includes various chaperone proteins. Indeed, the mitochondria-localized Hsp60 is rapidly upregulated and/or released from the mitochondria to the cytosol in response to the three apoptotic stimuli (Chandra *et al*., 2002). Finally, CKIs such as $p27^{KIP1}$ and $p21^{WAF-1}$ may also represent prosurvival molecules as cell-cycle-arrested cells generally survive better than proliferating cells. For example, $p21^{WAF-1}$ is a critical prosurvival factor transactivated by p53 and its inactivation sensitizes cells to apoptosis (Javelaud and Besancon, 2002).

It is unlikely that the induction of prosurvival molecules by apoptotic stimuli will be limited to the apoptotic inducers studied here. Indeed, many chemotherapeutic drugs (e.g., camptothecin, teniposide), chemopreventives (e.g., butyrate, short-chain fatty acids, PPAR$\gamma$ agonists, retinoids), chemicals (e.g., Mn, NDGA), and apoptosis inducers (e.g., Fas, hypoxia) have been shown to induce early mitochondrial activation, characterized by cytochrome *c* upregulation and increased mitochondrial respiration (Chandra *et al*., 2002 and references therein). Similarly, hypoxia selectively upregulates Bcl-$X_L$, leading to generation of death-resistant cells (Dong and Wang, 2004). UV irradiation eliminates Mcl-1 but also induces increased targeting of Bcl-$X_L$ to mitochondria (Nijhawan *et al*., 2003). Finally, many apoptotic stimuli rapidly upregulate SODs, heat-shock proteins, and other prosurvival molecules (Kinnula and Crapo, 2003). Therefore, induction of prosurvival mechanisms by apoptotic stimuli might represent a general phenomenon. Even apoptosis induced by TNF$\alpha$ (Micheau and Tschopp, 2003) and the death kinase PKR (Donze *et al*., 2004) is preceded by an early phase of NF-$\kappa$B-mediated prosurvival signaling, which delays apoptosis. The induced prosurvival molecules apparently play a causal role in extending cell survival, as prevention of the induction of Bcl-2, Bcl-$X_L$, or MnSOD by apoptotic stimuli accelerates cell death.

The induction of both prosurvival and prodeath molecules by apoptotic stimuli occurs at the transcriptional level, thus implicating transcription factors. By focusing our initial effort on FOXO3a, we demonstrate the role of FOXO3a in regulating Bim and MnSOD, two molecules previously shown to contain the FOXO3a sites in their promoter regions and thus represent the direct transcriptional targets of FOXO3a. Experiments using $FOXO3a^{-/-}$ MEFs indicate that MnSOD upregulation requires FOXO3a, whereas the transcriptional activation of Bim may only partially depend on FOXO3a. Interestingly, several other prosurvival molecules including Cu/ZnSOD, Bcl-2, Bcl-$X_L$, and

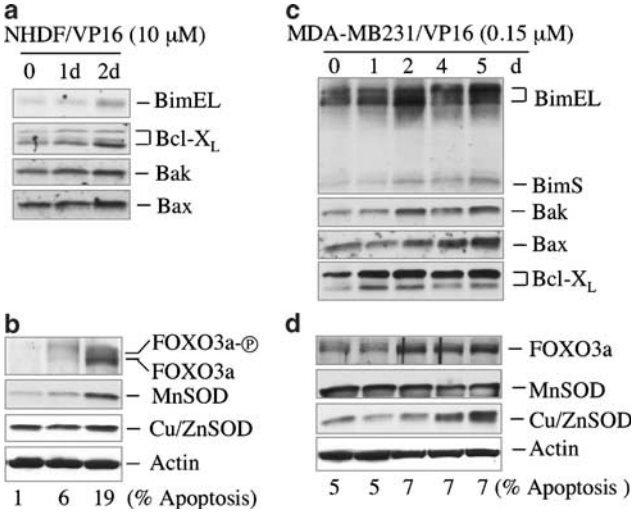


**Figure 7** Induction of FOXO3a and prosurvival and prodeath molecules in NHDF cells and at non-apoptotic conditions. (**a, b**) NHDF were treated with VP16 (10 $\mu$M). At the end, cells were harvested and whole-cell lysates (30 $\mu$g/lane) were used for Western blotting or scored for apoptosis. (**c, d**) MDA-MB231 cells were treated with a low concentration of VP16 (0.15 $\mu$M) for the time intervals indicated. At the end, cells were harvested for Western blotting and scored for apoptosis

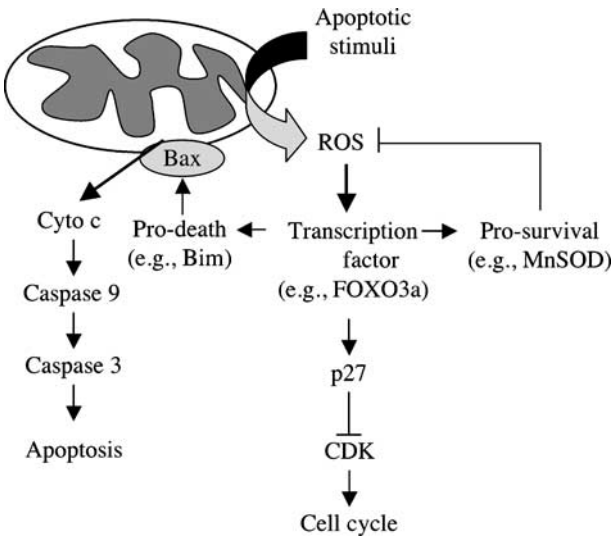


**Figure 8** A schematic depicting that cells respond to various apoptotic stimuli by rapidly generating ROS in the mitochondria, which activate master transcription factors such as FOXO3a, which in turn transcriptionally activate both prosurvival and prodeath molecules

cytochrome *c* also appear to be partially regulated by FOXO3a as their induction is also partially inhibited by DN FOXO3a constructs or FOXO3a siRNA or in FOXO3a$^{-/-}$ fibroblasts. Whether FOXO3a directly or indirectly regulates these molecules remains to be determined. Other transcription factors such as p53, E2F1, c-myc, and NF$\kappa$B, and signaling molecules such as ERK (Nair *et al*., 2004), may also be involved in the transcriptional activation of both pro and antiapoptotic molecules in response to apoptotic stimulation.

In our studies, three apoptotic stimuli with distinct mechanisms of action all upregulate FOXO3a itself at the transcriptional level. Several lines of evidence suggest that ROS appear to function as critical apical signaling molecules to activate FOXO3a and perhaps other multifunctional transcription factors (Figure 8). First, there is early mitochondrial activation, which is generally accompanied by increased ROS generation. Indeed, increased ROS are detected early upon stimulation in all three apoptotic systems. Second, many of the induced antiapoptotic molecules, including cytochrome *c*, Bcl-2, Bcl-$X_L$, and SODs, are related to or induced by oxidative stress, raising the possibility that these molecules are induced by slightly increased ROS early during apoptotic stimulation to guard against further increases in ROS (Figure 8). Third, importantly, suppression of ROS generation by ROS inhibitors/scavengers inhibits apoptotic-signal-induced upregulation of FOXO3a, as well as of its prodeath and prolife targets. Conversely, artificially generated oxidative stress upregulates FOXO3a and its targets. Fourth, that ROS function as signaling molecules that activate multifunctional transcription factors and ultimately determine the life and death of a cell is consistent with the well-established dual functions of ROS. Finally, FOXO3a and several other transcription factors, including NF$\kappa$B and p53, are well known to be regulated by and also respond to oxidative stress (Finkel and Holbrook, 2000; Nemoto and Finkel, 2002). For example, enforced expression of FOXO3a has been shown to confer resistance to oxidative stress (Nemoto and Finkel, 2002) and protect quiescent cells from oxidative stress (Kops *et al*., 2002).

How ROS activate the FOXO3a is unclear at present. FOXO3a is phosphorylated by Akt, which is a downstream target of ROS (Brunet *et al*., 1999). Recently, FOXO3a has been found to form a complex with SIRT1 (a mammalian homolog of the longevity gene Sir2) in response to oxidative stress (Brunet *et al*., 2004). By deacetylating FOXO3a, SIRT1 increases FOXO3a's ability to induce cell-cycle arrest and resistance to oxidative stress. Newly emerged evidence also makes the connection between FOXO3a and NF$\kappa$B, the best-studied transcription factor mediating cell survival. One study suggests that I$\kappa$B kinase (IKK) inhibits FOXO3a through physical interaction and phosphorylation independent of Akt, which promotes FOXO3a proteolysis via the Ub-dependent proteasome pathway (Hu *et al*., 2004). The other study suggests that FOXO3a negatively regulates NF$\kappa$B and FOXO3a deficiency results in NF$\kappa$B hyperactivation and T-cell hyperactivity (Lin *et al*., 2004). These new findings, together with our present results, suggest that FOXO3a is intricately regulated by multiple signaling pathways and FOXO3a, like NF$\kappa$B, represents one of the most important molecules dictating whether a cell lives or dies in response to stress.

Our observations lead us to propose a model in which apoptotic stimuli cause an early mitochondrial activation, leading to rapid generation of ROS (Figure 8). The ROS then activate master transcription factors such as FOXO3a, which in turn directly or indirectly activate multiple target genes, with either proapoptotic or antiapoptotic functions. This model is applicable to normal cells, as well as to transformed and cancer cells. The signaling pathways proposed seem to be activated as soon as cells sense stress, independent of how great the stress and whether or not the final outcome is cell death. It seems that the strengths and timings of the various prosurvival and prodeath signals determine the ultimate fate of the stressed cell. Presumably, by integrating these signals the cell can sensitively decide whether it should continue to live or kill itself.

This model (Figure 8) has the following implications. First, because apoptotic stimuli activate both prodeath and prosurvival molecules, the sensitivity of any target cells, for example, cancer cells receiving treatments, to apoptosis induction perhaps will be dictated by the balance of these two opposing signals. Furthermore, prosurvival molecules may be induced prior to induction of prodeath molecules (e.g., Figures 6c and 7c). These considerations suggest that significant cell killing occurs when, and *only when*, proapoptotic signals overwhelm (e.g., by the persistent apoptotic stimulation) the prosurvival signals or when the latter are eliminated.

Second, because cells in a tumor respond to apoptotic stimulation asynchronously and differently, some cells may preferentially upregulate prosurvival molecules, rendering them relatively resistant to further apoptotic stimulation. Finally, these observations suggest that the most effective anticancer therapies may be those that both promote apoptosis and suppress prosurvival mechanisms.

## Materials and methods

### *Cells culture and reagents*

LNCaP, MDA-MB231, and GM701 cells were cultured in serum-containing media. NHDF and its medium were bought from Clonetics. FOXO3a$^{+/+}$ and FOXO3a$^{-/-}$ MEFs (Castrillon *et al*., 2003) were courtesy of Dr R DePinho. Primary antibodies were: monoclonal antiactin (ICN), monoclonal anti-Bad and polyclonal anti-Bak, Bax and p27 (Santa Cruz), monoclonal anti-Bcl-2 and cytochrome *c*, and rabbit anti-Bcl-x (BD PharMingen), rabbit anti-Bim (Calbiochem), rabbit anti-MnSOD and Cu/ZnSOD (Stressgen), rabbit anti-FOXO3a and FOXO3a$^{T32}$ (Upstate), and rabbit anti-Caspase-3 (Biomol). Dihydrorhodamine 123 (DHR123) and dihydroethidium were bought from Molecular Probes. All other chemicals were purchased from Sigma unless specified otherwise.

### *Subcellular fractionation and Western blotting*

Subcellular fractionation was carried out as described (Chandra *et al*., 2002, 2004; Chandra and Tang, 2003). Protein concentration was determined using MicroBCA kit (Pierce, Rockford, IL, USA). Western blotting was performed using enhanced chemiluminescence and the blot was stripped and reprobed (Liu *et al*., 2002) for proteins indicated in the Results.

### *Measurement of apoptosis*

Apoptosis was qualitatively (caspase-3 activation, PARP cleavage assays, DEVDase and LEHDase activity measurement, and DNA fragmentation) and quantitatively (fluorescence microscopy upon DAPI or annexin V-FITC staining) analysed as previously detailed (Tang *et al*., 1998; Chandra *et al*., 2002, 2004; Liu *et al*., 2002).

### *RT–PCR*

Total RNA was isolated using Tri-reagent (Invitrogen). RT was performed using 2 $\mu$g of total RNA (at 42°C for 2 h) in a total 20 $\mu$l volume containing random hexamers and Superscript II reverse transcriptase (Invitrogen). For PCR, 1 $\mu$l of cDNA was used in a 50-$\mu$l reaction containing 1 $\mu$M primers (primer information is available upon request), dNTPs and *Taq*, using the cycling profile 94°C × 30 s, 60°C × 30 s, and 72°C × 30 s for 25 cycles.

### *ROS measurement by flow cytometry*

ROS were measured using cell-permeable dyes DHR123 or dihydroethidium (Tang and Honn, 1997; Joshi *et al*., 1999). DHR123 primarily binds to $H_2O_2$ whereas dihydroethedium primarily binds to $O_2^{\bullet -}$. For staining, DHR123 or dihydroethedium was preloaded into cells for 20 min before LNCaP, MDA-MB231, or GM701 cells were treated with apoptotic stimuli. Samples were analysed on a Coulter Epics Elite flow cytometer. In all, 20 000 viable cells were measured per sample, and cell debris and cell aggregates were electronically gated out. The results were expressed as mean log fluorescence intensity. The experiments were repeated three times.

### *siRNA downregulation of Bim, Bcl-2, Bcl-$X_L$, MnSOD, and FOXO3a*

Bcl-2 siRNA (GCUGCACCUGACGCCCUUCTT) and Bcl-$X_L$ siRNA (CAGGGACAGCAUAUCAGAGTT) (Jiang and Milner, 2003) and the control siRNA (GUCAGCCUCAC GCGCCCUUTT), and Bim siRNA (AAGGUAGACAA UUGCAGCCUG) were chemically synthesized (Ambion, Austin, TX, USA). MnSOD siRNA (AAAUUGCUGCUUG TCCAAAUC), FOXO3a siRNA (AAUGUGACAUGGA-GUCCAUUA), and the control siRNA (GUCAGCCUCAC GCGC CCUUTT) were synthesized using the *Silencer*™ siRNA Construction Kit (Ambion). Cells cultured in 3.5 cm dishes ($1 \times 10^5$ cells/dish) were either untransfected or transfected with the control or siRNA oligos at a final concentration of 60 nM using siPORT-Lipid (Ambion). About 24–48 h after transfection, cells were treated with apoptotic stimuli for various time intervals. At the end of treatments, cells were harvested for Western blotting or analysed for apoptosis.

### *Relationship between FOXO3a, Bim, and MnSOD induction during apoptosis*

LNCaP cells were plated in 6 cm culture dishes. At 40–60% confluence, cells were transfected with either plasmids encoding two forms of dominant-negative FOXO3a by FuGENE6, or FOXO3a siRNA. Cells were subjected to starvation next day and harvested after 24 h treatment. In another set of experiments, FOXO3a$^{+/+}$ or FOXO3a$^{-/-}$ MEFs cultured in 6-cm dishes were treated with VP16 (25 $\mu$M) or BMD188 (40 $\mu$M). Cells were harvested at different time points for protein analysis.

### *Effect of ROS generation on Bim, FOXO3a, and MnSOD expression*

LNCaP cells at 40–60% density were pretreated with ROS inhibitors including NAC, mannitol, or GSH all at 1 mM for 1.5 h (Tang and Honn, 1997). Then cells were subjected to serum starvation for 8 and 24 h, after which cells were harvested for Western blotting. LNCaP cells were also treated with $H_2O_2$ at 1 mM for 6 h and then used to measure the levels of these proteins.

**Acknowledgements**
We thank R DePinho for FOXO3a$^{+/+}$ and FOXO3a$^{-/-}$ MEFs, Biomide Corp. for BMD188, K Claypool for flow analysis, M Raff for advice and critically reading the manuscript, and the Tang lab for support. This work was supported, in part, by NIH Grants CA90297 and AG023374, ACS Grant RSG MGO-105961, DoD Grant DAMD17-03-1-0137, and NIEHS Center Grant 5 P30 ES07784 (all to DGT), and DoD Postdoctoral Fellowships DAMD17-03-1-0146 (J-WL) and DAMD17-02-1-0083 (DC).

## References

Adler V, Yin Z, Tew KD and Ronai Z. (1999). *Oncogene*, **18,** 6104–6111.
Birkenkamp KU and Coffer PJ. (2003). *J. Immunol.*, **171,** 1623–1629.
Bouillet P, Purton JF, Godfrey DI, Zhang LC, Coultas L, Puthalakath H, Pellegrini M, Cory S, Adams JM and Strasser A. (2002). *Nature*, **415,** 922–926.
Brunet A, Bonni A, Zigmond MJ, Lin MZ, Juo P, Hu LS, Anderson MJ, Arden KC, Blenis J and Greenberg ME. (1999). *Cell*, **96,** 857–868.
Brunet A, Sweeney LB, Sturgill JF, Chua KF, Greer PL, Lin Y, Tran H, Ross SE, Mostoslavsky R, Cohen HY, Hu LS, Cheng H-L, Jedrychowski MP, Gygi SP, Sinclair DA, Alt FE and Greenberg ME. (2004). *Science*, **303,** 2011–2015.
Castrillon DH, Miao L, Kollipara R, Horner JW and DePinho RA. (2003). *Science*, **301,** 215–218.
Chandra D, Choy G, Deng X, Bhatia B, Daniel P and Tang DG. (2004). *Mol. Cell. Biol.*, **24,** 6592–6607.
Chandra D, Liu JW and Tang DG. (2002). *J. Biol. Chem.*, **277,** 50842–50854.
Chandra D and Tang DG. (2003). *J. Biol. Chem.*, **278,** 17408–17420.
Danial NN and Korsmeyer SJ. (2004). *Cell*, **116,** 205–219.
Dijkers PF, Birkenkamp KU, Lam EW-F, Thomas NSB, Lammers J-W, Koenderman L and Coffer PJ. (2002). *J. Cell Biol.*, **156,** 531–542.
Dijkers PF, Medema RH, Lammers JW, Koenderman L and Coffer PJ. (2000). *Curr. Biol.*, **10,** 1201–1204.
Dong Z and Wang J. (2004). *J. Biol. Chem.*, **279,** 9215–9221.
Donze O, Deng J, Curran J, Sladek R, Picard D and Sonerberg N. (2004). *EMBO J.*, **23,** 564–571.
Finkel T and Holbrook NJ. (2000). *Nature*, **408,** 239–247.
Gilley J, Coffer PJ and Ham J. (2003). *J. Cell Biol.*, **162,** 613–622.
Hockenbery DH, Oltavai ZN, Ying XM, Milliman CL and Korsmeyer SJ. (1993). *Cell*, **75,** 241–251.
Hu MC, Lee DF, Xia W, Golfman LS, Ou-Yang F, Yang JY, Zou Y, Bao S, Hanada N, Saso H, Kobayashi R and Hung MC. (2004). *Cell*, **117,** 225–237.
Huang H-L, Fang L-W, Lu S-P, Chou C-K, Luh T-Y and Lai M-Z. (2003). *Oncogene*, **22,** 8168–8177.
Javelaud D and Besancon F. (2002). *J. Biol. Chem.*, **277,** 37949–37954.
Jiang M and Milner J. (2003). *Genes Dev.*, **17,** 832–837.
Joshi B, Li L, Taffe BG, Zhu Z, Wahl S, Tian H-S, Ben-Josef E, Taylor JD, Porter AT and Tang DG. (1999). *Cancer Res.*, **59,** 4343–4355.
Kinnula VL and Crapo JD. (2003). *Am. J. Respir. Crit. Care Med.*, **167,** 1600–1619.
Kops GJPL, Dansen TB, Polderman PE, Saarloos I, Wirtz KWA, Coffer PJ, Huang T-T, Bos JL, Medema RH and Burgering BMT. (2002). *Nature*, **419,** 316–321.
Lin L, Hron JD and Peng SL. (2004). *Immunity*, **21,** 203–213.
Liu JW, Chandra D, Tang SH, Chopra D and Tang DG. (2002). *Cancer Res.*, **62,** 2976–2981.
Martin AG and Fearnhead HO. (2002). *J. Biol. Chem.*, **277,** 50834–50841.
Micheau O and Tschopp J. (2003). *Cell*, **114,** 181–190.
Mikkelsen RB and Wardman P. (2003). *Oncogene*, **22,** 5734–5754.
Modur V, Nagarajan R, Evers BM and Mildbrandt J. (2002). *J. Biol. Chem.*, **277,** 47928–47937.
Nair VD, Warren TYC, Olanow W and Sealfon SC. (2004). *J. Biol. Chem.*, **279,** 27494–27501.
Nemoto S and Finkel T. (2002). *Science*, **295,** 2450–2452.
Nijhawan D, Fang M, Traer E, Zhong Q, Gao W, Du F and Wang X. (2003). *Genes Dev.*, **17,** 1475–1486.
Plas DR and Thompson CB. (2003). *J. Biol. Chem.*, **278,** 12361–12366.
Putcha GV, Moulder KL, Golden JP, Bouillet P, Adams JA, Strasser A and Johnson EM. (2001). *Neuron*, **29,** 615–628.
Raff MC. (1992). *Nature (London)*, **356,** 397–400.
Ramaswamy S, Nakamura N, Sansi I, Bergeron L and Sellers WR. (2002). *Cancer Cell*, **2,** 81–91.
Ricci J-E, Gottlieb RA and Green DR. (2003). *J. Cell Biol.*, **160,** 65–75.
Rokudal S, Fujita N, Kitahara O, Nakamura Y and Tsuruo T. (2002). *Mol. Cell. Biol.*, **22,** 8695–8708.
Sade H and Sarin A. (2004). *Cell Death Differ.*, **11,** 416–423.
Schimidt M, de Mattos SF, van der Horst A, Klompmaker R, Kops GJPL, Lam EW-F, Burgering BMT and Medema RH. (2002). *Mol. Cell. Biol.*, **22,** 7842–7852.
Sundaresan M, Yu ZX, Ferrons VJ, Irani K and Finkel T. (1995). *Science*, **270,** 296–299.
Tang DG and Honn KV. (1997). *J. Cell. Physiol.*, **172,** 155–170.
Tang DG, Li L, Chopra DP and Porter AT. (1998). *Cancer Res.*, **58,** 3466–3479.
Valks DM, Kemp TJ and Clerk A. (2003). *J. Biol. Chem.*, **278,** 25542–25547.
Zhao Y, Wang Z-B and Xu J-X. (2003). *J. Biol. Chem.*, **278,** 2356–2360.